X-ray determinations of the liquid-structure factor and pair-correlation function of ^{4}He

F. H. Wirth* and R. B. Hallock
Laboratory for Low Temperature Physics, Department of Physics and Astronomy, University of Massachusetts, Amherst, Massachusetts 01003
(Received 9 January 1986)

Measurements of the intensity of Cu $K\alpha$ x rays scattered from liquid ^{4}He as a function of temperature and pressure are used to determine the liquid-structure factor and pair-correlation function of the fluid. Data are reported for $1.16 \leq T \leq 3.5$ K at the three densities 150.3, 162.5, and 171.0 kg/m^3. Earlier data of Robkoff and Hallock are reanalyzed and found to be in excellent agreement with our new results. The temperature dependence of the structure factor at fixed density is in good agreement with predictions based on the thermal population of rotons due to Reatto and co-workers.

I. INTRODUCTION

The spatial structure of ^{4}He as it passes through its superfluid transition has been a focus of interest and studied by both x-ray and neutron scattering for many years. The early work of Henshaw[1] clearly showed an anomalous behavior in the temperature dependence of the spatial order on cooling below T_λ. More recent work,[2–8] both with x rays and neutrons has explored this temperature dependence more carefully. We present here the results of a series of measurements of the structure factor, $S(k)$, of liquid helium at three fixed densities (150.29, 162.47, and 171.0 kg/m^3) and in the temperature range $1.16 \leq T \leq 3.5$ K.

In Sec. II we briefly describe the apparatus used for these measurements. In Sec. III we describe our procedure in detail. Sections IV and V contain our results for the liquid-structure factor and the pair-correlation function as well as a discussion of the relevance of several theoretical ideas which have been proposed to explain the loss of spatial structure seen on cooling ^{4}He below T_λ. In Sec. VI we compare these data to earlier data collected in this laboratory. Section VII is reserved for summary and conclusions.

II. APPARATUS

All measurements reported here were made on an automated x-ray diffractometer with cryogenic capabilities that has been previously described in the literature.[9] We will include here a summary description of the apparatus adequate to allow an understanding of our approach. Several modifications made since the apparatus was last described will be mentioned.

The intense x-ray beam necessitated by the relatively small scattering coefficient of helium is provided by a 12-kW water-cooled rotating anode x-ray generator.[10] An electron beam of 50 kV at 160 mA was employed to generate the Cu $K\alpha$ x rays for all of the work reported here. Improvements in the water and oil seals of the rotating anode resulted in beam intensities that varied less than 1% during a typical 8-h run of data acquisition. These variations in intensity had the form of a monatonic decrease in overall beam intensity with an occasional step-function increase caused by the servomechanisms controlling beam current and voltage. The anode is copper and provides enhanced intensity at the characteristic $K\alpha$ and $K\beta$ lines near 1.54 Å. The line focus of this anode combined with a system of slits and Soller slits creates a beam of rectangular cross section 10×2 mm^2 with the longer dimension vertical and with a divergence of 0.3° in the horizontal plane. This beam intersects a vertically oriented 0.95-cm-diam right circular cylinder sample chamber midway in its 2.5 cm height. This chamber is made of high-purity beryllium[11] with a wall thickness of 0.25 mm and is incorporated in a continuously filled ^{4}He cryostat which allows continuous operation at temperatures $T \gtrsim 1.16$ K. Heat shields anchored at 4 and 77 K surround the sample chamber and help to maintain an isothermal environment.

The scattered x rays are collimated to a horizontal divergence of 0.3° by a similar set of slits and Soller slits mounted in a movable detector arm. A high-purity germanium detector[12] (HPGE) provides the energy discrimination necessary for this experiment. [The resolution of 284-eV full width at half maximum (FWHM) at 1.54 Å is adequate to easily separate the $K\alpha$ and $K\beta$ lines.] The detector arm can be rotated around the axis of the sample chamber by a goniometer[13] and positioned with an accuracy of 0.01° relative to the incident beam axis. Beryllium windows in the vacuum jacket and thermal shields of the cryostat system allow a 150° unobstructed view of the sample chamber, 30° on one side of the beam direction and 120° on the other. The incident beam enters the apparatus through its own, smaller beryllium windows. The overall configuration of the apparatus[9] is shown in Fig. 1. The scattered x rays that do not enter the detector arm of the apparatus are blocked by a flexible shield of interlocking hinged lead plates that allows the detector arm freedom of movement. Improvements in the suspension of these plates has given them a more uniform motion and reduced binding.

A major change in the configuration of the apparatus was the incorporation of a beam stop inside the movable lead shielding. This was simply constructed from a 2-mm-thick lead sheet and secured over the exit window of

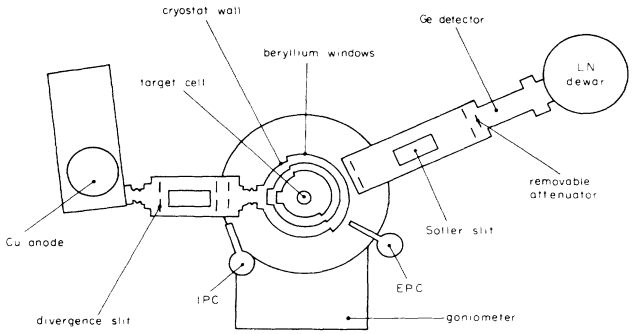

FIG. 1. Schematic diagram of the x-ray diffractometer (Ref. 9).

the cryostat in a position so as to intercept the unscattered main x-ray beam as it leaves the apparatus. The reasons for this modification will be discussed later.

In addition to the germanium crystal detector, two Xe-CO_2 proportional counters[14] are incorporated into the apparatus to monitor the incident beam intensity and the intensity of radiation scattered by the sample at a fixed angle. These will be referred to as the incident proportional counter (IPC) and the exit proportional counter (EPC), respectively. Pulse-height spectra from the HPGE and EPC were obtained on a 1024-channel multichannel analyzer (MCA). The IPC signal was windowed by means of a single-channel analyzer and recorded digitally.

The operation of the diffractometer and the short-term storage and rudimentary manipulation of the data were controlled by an Apple II^+ computer. Major analysis of the complete data set was done on a Cyber 175/720 system. Our data file consisted of the temperature and pressure of the gas or liquid being studied, the IPC reading at the beginning and end of each run (to monitor the main beam), the Fe $K\alpha$, Cu $K\alpha$, Cu $K\beta$, and EPC integrated peak intensities at each angle as well as the raw data at all angles of interest.

III. PROCEDURES

Ideally one can calculate the structure factor form

$$I(k)=AN(k)T[\sigma_e(k)S(k)+\sigma_i(k)] , \tag{1}$$

where A is the Thompson scattering factor, N is the number of scattering centers, T is a transmission coefficient that accounts for absorption, σ_e is the coherent scattering factor, σ_i the inelastic scattering factor, $I(k)$ is the scattered intensity and $k=(4\pi/\lambda)\sin(\theta/2)$, λ is the x-ray wavelength, and θ is the scattering angle. The main obstacle to this prescription in an experiment of this sort is the difficulty of knowing $N(k)$ as a function of scattering angle.

We address this problem by scattering off an ideal gas (neon at 77 K and 1 atm whose structure factor is very nearly unity) following a method employed earlier by Tweet.[15] We can solve for the structure factor of the helium in this context and obtain

$$S(k)=\frac{T_{\mathrm{Ne}}\rho_{\mathrm{Ne}}I_{\mathrm{He}}(\sigma_{i\mathrm{Ne}}+\sigma_{e\mathrm{Ne}})}{T_{\mathrm{He}}\rho_{\mathrm{He}}I_{\mathrm{Ne}}\sigma_{i\mathrm{He}}}+\frac{\sigma_{i\mathrm{He}}}{\sigma_{i\mathrm{Ne}}} . \tag{2}$$

Here the subscripts Ne and He refer to neon and helium, respectively. The transmission factors are calculated along the cell diameter by $T=e^{-\mu d\rho}$, where μ is the mass absorption coefficient, ρ the density, and d the cell diameter. Helium densities are interpolated from tables due to Elwell and Meyer[16] and Maynard.[17] Neon densities are determined from an equation of state.[18] We find the coherent and incoherent scattering factors by interpolation of the tables due to Tovard *et al.*[19] for neon and tables due to Kim and Inokuti[20] for helium. The incoherent cross sections are then corrected for relativistic recoil.

Before the experimental intensities can be used in Eq. (2) they must be corrected in a number of ways: A correction for pulse pileup is necessitated since a mixer-router is utilized to incorporate both HPGE and EPC data in the partitioned memory of the MCA, and simultaneous counts are rejected. The two count rates R_1 and R_2 and the dead times associated with the device t_1, t_2 for the HPGE and EPC detectors, respectively, can be related to the corrected rates R_1' and R_2' by

$$\begin{aligned} R_1'&=R_1(1-R_2\{t_1\exp[-R_2t_1+t_2\exp(-R_1t_2)]\}) ,\\ R_2'&=R_2(1-R_1\{t_2\exp[-R_1t_2+t_1\exp(-R_2t_1)]\}) . \end{aligned} \tag{3}$$

In our case the exponential terms are ~ 1.0 which simplifies the calculation. The data were normalized for a standard dwell time per channel and the natural background was subtracted. When more than one set of data was used, each set was normalized in overall intensity by comparison to the first data set of the group and then averaged.

We had the option of normalizing any data set by an overall intensity factor determined by the IPC reading and of intrascan normalizations via the EPC reading. As we shall describe, neither of these options were reliable over the full course of these measurements. The IPC counts did not consistently reflect changes in intensity monitored by the GE detector and the EPC readings had a nonreproducible dependence on the location of the detector arm, especially at large angles. We believe the first of these problems may be due to the inability of the CO_2-Xe proportional counters to separate the Fe $K\alpha$ and Cu $K\alpha$ lines. Thus, changes in intensity as a function of wavelength in the primary beam particularly at high energies were reflected in the relative amount of iron fluorescence and added unwanted counts to the IPC and EPC.

We noticed that both the IPC and EPC readings were much stronger functions of beam voltage than those of the germanium detector. Also, the energy spectra of these counters showed considerable variability in the wavelength region near the Fe $K\alpha$ peak. In addition, brass absorbers were sometimes used (75 μm shimstock) in front of the EPC counter to attenuate the incident radiation when relatively high count rates were encountered (principally for liquid-helium samples). These absorbers selectively attenuated the Fe $K\alpha$ line. With the absorbers in place, the EPC behaved in a much more tractable manner, all the problems mentioned above being considerably reduced, but not eliminated. The angular dependence of the EPC probably has two causes: scattering of the primary

beam from the lead shields and physical interference of the shields with the collimation assembly of the EPC. The insertion of a lead beam stop alleviated the problem to some degree, but not enough to make the normalization data fully reliable. Fortunately, following improvements in the anode seals, neither correction was ultimately necessary because of the relatively stable anode performance encountered during the data collection; intensities varied by no more than 3% over the entire course of data collection. Although some of these corrections were appropriate to earlier work done in this laboratory,[3,4] none were used for any of the work presented here.

In addition to helium- and neon-scattering data, empty cell scattering data at both 77 and 4 K were obtained. These were subtracted from the neon and helium data, respectively, taking into account transmission losses from the filled cell. A correction was made for multiple scattering in the helium data; the multiple-scattering effect in neon is negligible. Following the procedure of Blech and Auerbach[21] we arrived at density dependent corrections on the order of 1%. This method is a very simple approximation, assuming the atoms to be elastic, incoherent, and isotropic scatterers, but the size of the correction justifies its use. Finally, the structure factor for each angle was calculated via Eq. (2).

Although the main beam was observed to be quite stable in intensity, it was a concern throughout the course of the experiment. Slow changes in the anode surface characteristics and day-to-day variations in the x-ray machine set points were known to cause intensity changes on the order of 1%. Since the IPC was not reliable, two methods were used to monitor these intensities. First, fiducial scans at a chosen temperature and density were repeated throughout the series of data runs. Normalization factors generated from the total counts in a selected region of these scans could be used to scale the intensities of all nearby data. Similarly, normalization factors could be generated for all empty cell and neon data. The neon and empty cell data was obtained repeatedly and applied to the helium scans in their temporal proximity.

We generated an internal scale factor by the criterion that the average value of $S(k)$ for $4.8 \lesssim k \lesssim 5.1$ Å^{-1} should be unity. $S(k)$ is not truly constant and equal to one in this range but the error generated by this approximation is small compared to the statistical uncertainties of our large momentum transfer data. This procedure does not introduce a systematic error in the vicinity of the main structure factor peak greater than $\sim 0.5\%$. Our confidence in this method is increased by the observation that this scale factor follows the known long-term behavior of the x-ray intensity. With few exceptions such scale factors indicated intensity variations of about $\sim 3\%$ over the course of the experiment and $\sim 0.5\%$ day to day.

IV. RESULTS

The results of our determinations of the liquid structure factor are displayed in Table I for the three densities considered, 150.29, 162.47, and 171.00 kg/m^3.

In order to facilitate further analysis, each of these structure factors was fit to three somewhat arbitrary multiparameter functions, a sixth-order polynomial for low k [that forced $S(k=0)$ to its thermodynamic value] the product of a linear, a quadratic, and a Gaussian term in the peak area and a sixth-order polynomial in the high-k region that required $S(k)$ to asymptote to unity. The functions were chosen both to give excellent standard deviations and to minimize systematic errors, especially in the region of the peak. In the transitional regions a weighted average of the overlapping functions was used. A typical structure factor and its fitted curve are shown in Fig. 2.

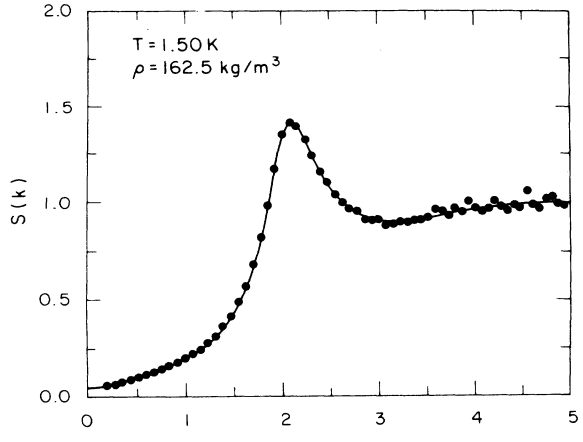

FIG. 2. A typical structure factor for $T=1.5$ K, $\rho=162.47$ kg/m^3. The solid curve is a fit to the data points as described in the text.

Since the height of the principal peak in the structure factor is a qualitative measure of the spatial order of the liquid helium, we determined this value and the location in momentum transfer of the maximum from the fitted curves. These data are presented in Table II and plotted in Figs. 3 and 4. At all three densities the maximum

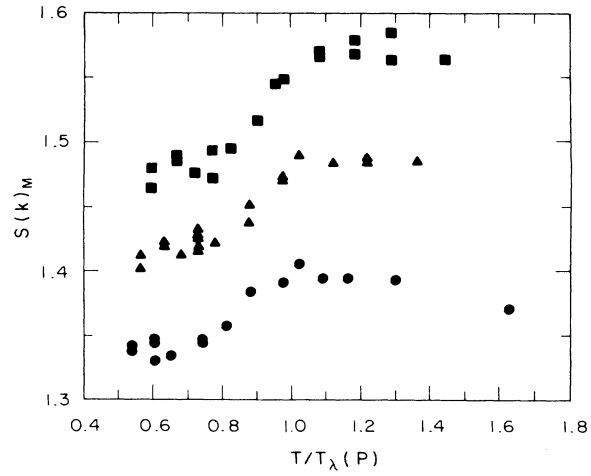

FIG. 3. The height of the principal peak in $S(k)$ versus reduced temperature (T/T_λ) for the three densities considered in this work: (●) 150.29, (▲) 162.47, and (■) 171.0 kg/m^3.

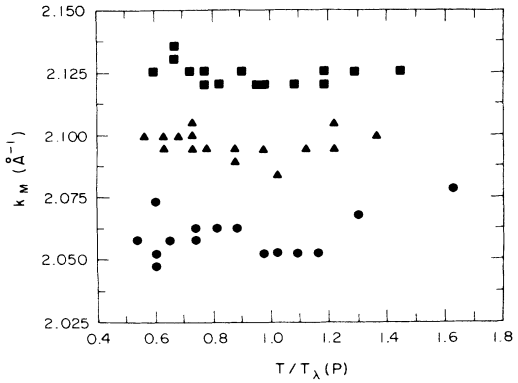

FIG. 4. Location in momentum transfer, k_M, of the principal peak in $S(k)$ versus reduced temperature (T/T_λ) for three densities: (●) 150.29, (▲) 162.47, and (■) 171.0 kg/m^3.

height of the principal peak in $S(k)$ is achieved in the neighborhood of T_λ. The relatively slow increase in the amplitude of the main peak observed in cooling down to T_λ is evidence of increased spatial order upon cooling. The more rapid falloff upon cooling below this temperature is an indication of more interesting behavior and we shall return to it shortly. Internal consistency of the present set of data is very good. Scans at $\rho=162.47$ kg/m^3, $T=1.5$ K were repeated at intervals throughout the entire data collection period. The peak heights generated from these data have a standard deviation of $\sim 0.5\%$.

Gaglione *et al.*[22] (GMR) have proposed that the behavior of the maximum of $S(k)$ as a function of temperature for $T<T_\lambda$ is due to the thermal excitation of rotons. The roton, being a relatively short-wavelength excitation, is expected to contribute to the short-range order

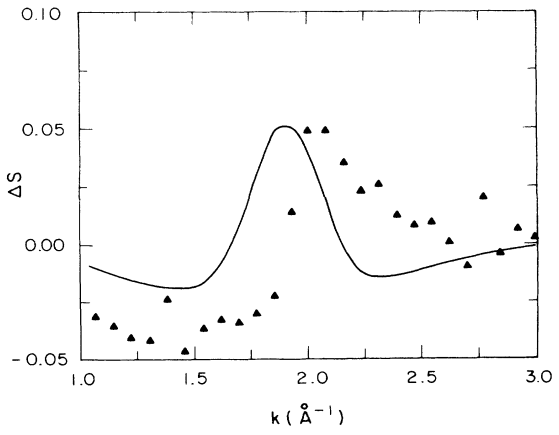

FIG. 5. $\Delta S=S(k,T=2.15$ K, $\rho=145$ kg/m$^3)-S(k,T=0$ K, $\rho=145$ kg/m$^3)$ plotted versus k after Gaglione *et al.* (Ref. 22) (solid line) compared with our data (△) $\Delta S(k,T=2.10$ K, $\rho=150.29$ kg/m$^3)-S(k,T=1.16$ K, $\rho=150.29$ kg/m$^3)$.

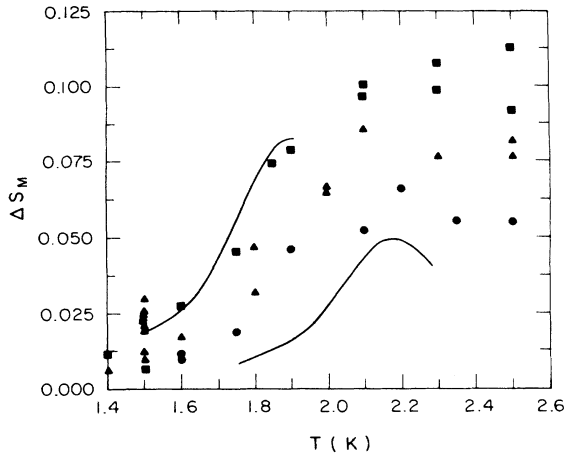

FIG. 6. The maximum value of $\Delta S=S(k,T,\rho)-S(k,T=0,\rho)$, ΔS_M as calculated by Gaglione *et al.* (Ref. 23) for the upper solid curve $\rho=174$ kg/m^3 and for the lower solid curve $\rho=145.0$ kg/m^3 compared with our values $\Delta S=S(k,T,\rho)-S(k,T=1.16$ K, $\rho)$ at three densities: (■) 171, (▲) 162.47, and (●) 150.29 kg/m^3.

of the liquid. GMR use a modified Penrose[23] density matrix to calculate the perturbation of the $T=0$ K structure factor due to the increasing population of rotons. In order to increase the validity of these calculations near T_λ they incorporate empirical expressions for the roton dispersion relation and energy linewidth. GMR suggest their derivation is rigorous up to ~ 1.7 K, that the experimental values for the roton energy play a role above this temperature and that the finite lifetime of roton states becomes important above 2 K. They further suggest that their predictions retain some validity above the λ point.

Values for $\Delta S(k,T)$ defined[24] as

$$\Delta S(k,T)=S(k,T)-S(k,T=0) \tag{4}$$

are reported by Gaglione *et al.*[22] for three values of the density, 145, 159.5, and 174 kg/m^3. Experimental values of the low-temperature structure factor[7] were used to develop the predictions of ΔS. A typical case for the specific choice $\rho=145$ kg/m^3 and $T=2.1$ K is shown in Fig. 5 together with experimental values from our data fits for $\Delta S(k)=S(k,\ T=2.1$ K$)-S(k,\ T=1.16$ K), at the closest experimental density of 150.29. Despite the large experimental uncertainties, it is clear that our data shows a very similar peak at a slightly larger value of the momentum transfer than the theoretical prediction.

Because the form of $\Delta S(k)$ is not a strong function of T or ρ, GMR only report values for its *maximum* at all the temperatures and densities they considered. These maxima, along with the maximum values of ΔS determined in this work are shown in Fig. 6. As can be seen, agreement is quite good, with GMR's high- and low-density curves (which bracket our experimental densities) generally enclosing our data points. In addition, GMR predict a small shift (to lower k) on the order of 0.015 Å^{-1}, in the location of the maximum of $S(k)$ as one warms toward T_λ. This appears to be due to the location

TABLE I. Structure values in this work for $\rho = 150.29$, 162.47, and 171.00 kg/m^3.

k \ T (K)	1.16	1.30	1.40	1.60	1.75	1.90
			$\rho = 150.29$ kg/m^3			
0.1867	0.0732	0.0598	0.0758	0.0630	0.0861	0.0708
0.2667	0.0838	0.0720	0.0855	0.0725	0.0914	0.0774
0.3466	0.0946	0.0862	0.0989	0.0854	0.1030	0.0866
0.4266	0.1144	0.1008	0.1143	0.0984	0.1175	0.1006
0.5065	0.1305	0.1148	0.1290	0.1124	0.1308	0.1116
0.5863	0.1463	0.1288	0.1450	0.1254	0.1481	0.1246
0.6661	0.1624	0.1441	0.1635	0.1394	0.1640	0.1397
0.7458	0.1816	0.1606	0.1807	0.1568	0.1821	0.1555
0.8254	0.1994	0.1808	0.1994	0.1763	0.2018	0.1762
0.9050	0.2199	0.2002	0.2172	0.1946	0.2206	0.1960
0.9845	0.2477	0.2213	0.2473	0.2168	0.2505	0.2177
1.0639	0.2725	0.2481	0.2685	0.2437	0.2722	0.2438
1.1431	0.3046	0.2772	0.3022	0.2710	0.3083	0.2737
1.2223	0.3422	0.3124	0.3402	0.3079	0.3410	0.3055
1.3014	0.3864	0.3565	0.3799	0.3516	0.3848	0.3524
1.3803	0.4203	0.4087	0.4207	0.4019	0.4211	0.4005
1.4591	0.4985	0.4665	0.4939	0.4619	0.4923	0.4621
1.5377	0.5710	0.5493	0.5676	0.5438	0.5658	0.5426
1.6162	0.6561	0.6451	0.6527	0.6412	0.6523	0.6390
1.6946	0.7734	0.7629	0.7708	0.7592	0.7681	0.7550
1.7728	0.9182	0.9100	0.9154	0.9000	0.9192	0.8993
1.8508	1.0768	1.0634	1.0636	1.0616	1.0773	1.0691
1.9286	1.2225	1.2100	1.2215	1.2113	1.2418	1.2371
2.0063	1.3236	1.3218	1.3198	1.3245	1.3350	1.3585
2.0837	1.3368	1.3365	1.3290	1.3436	1.3570	1.3806
2.1610	1.3074	1.3073	1.3022	1.3155	1.3175	1.3473
2.2380	1.2533	1.2556	1.2416	1.2617	1.2474	1.2761
2.3149	1.1729	1.1874	1.1647	1.1837	1.1716	1.1992
2.3915	1.1145	1.1257	1.1033	1.1212	1.1066	1.1309
2.4679	1.0682	1.0776	1.0581	1.0784	1.0632	1.0971
2.5440	1.0120	1.0261	1.0007	1.0261	1.0123	1.0340
2.6199	0.9872	0.9949	0.9765	0.9897	0.9792	1.0073
2.6956	0.9671	0.9620	0.9624	0.9558	0.9672	0.9549
2.7709	0.9382	0.9534	0.9309	0.9513	0.9344	0.9599
2.8461	0.9168	0.9045	0.9173	0.9026	0.9228	0.9182
2.9209	0.9118	0.9158	0.9038	0.9129	0.9084	0.9389
2.9955	0.9046	0.9069	0.8980	0.9118	0.9115	0.9321
3.0697	0.8931	0.9000	0.8816	0.8990	0.8833	0.9148
3.1437	0.8682	0.8966	0.8740	0.8940	0.8713	0.9276
3.2174	0.8880	0.9044	0.8647	0.8989	0.8961	0.9085
3.2907	0.8975	0.9032	0.8949	0.9062	0.9042	0.9216
3.3638	0.9005	0.9215	0.8941	0.9158	0.9036	0.9369
3.4365	0.9137	0.9317	0.8974	0.9238	0.9338	0.9534
3.5089	0.9185	0.9423	0.8988	0.9354	0.9233	0.9475
3.5810	0.9576	0.9642	0.9469	0.9660	0.9539	0.9723
3.6527	0.9261	0.9630	0.9124	0.9733	0.9336	0.9872
3.7240	0.9749	0.9366	0.9552	0.9407	0.9707	0.9655
3.7950	1.0051	0.9633	0.9948	0.9486	1.0233	0.9887
3.8656	0.9641	0.9564	0.9719	0.9637	0.9863	0.9733
3.9359	1.0182	0.9940	0.9886	0.9814	1.0582	1.0169
4.0058	0.9497	0.9798	0.9371	0.9639	0.9554	0.9781
4.0753	1.0133	0.9610	0.9726	0.9592	0.9927	0.9871
4.1444	0.9332	0.9609	0.9275	0.9908	0.9386	0.9743
4.2131	1.0351	0.9945	1.0345	0.9853	1.0341	1.0370
4.2814	0.9931	0.9680	1.0049	0.9647	1.0214	0.9664
4.3493	0.9944	0.9457	0.9746	0.9320	1.0132	0.9630
4.4167	0.9783	0.9675	0.9759	0.9759	0.9741	0.9783
4.4837	0.9862	0.9671	0.9768	0.9349	1.0163	0.9964

TABLE I. (*Continued*).

k \ T (K)	1.16	1.30	1.40	1.60	1.75	1.90
			$\rho = 150.29$ kg/m^3			
4.5504	1.0269	1.0390	1.0295	1.0192	1.0297	1.0695
4.6165	0.9561	0.9752	0.9414	0.9490	0.9349	0.9847
4.6822	1.0050	0.9823	0.9796	0.9764	1.0172	1.0023
4.7475	0.9703	1.0080	0.9876	0.9988	0.9617	1.0671
4.8123	1.0282	1.0044	0.9730	1.0058	0.9868	0.9834
4.8767	1.0115	0.9918	1.0572	1.0069	1.0640	1.0279
4.9406	0.9639	0.9830	0.9553	1.0072	0.9490	0.9958
5.0040	1.0148	0.9949	1.0144	0.9897	1.0309	1.0077
5.0669	0.9938	1.0157	1.0052	0.9944	0.9862	1.0037

k \ T (K)	2.10	2.20	2.35	2.50	2.80	3.50
			$\rho = 150.29$ kg/m^3			
0.1867	0.0777	0.0805	0.0877	0.0901	0.0977	0.1381
0.2667	0.0825	0.0854	0.0902	0.0932	0.0996	0.1307
0.3466	0.0912	0.0949	0.0984	0.0998	0.1039	0.1335
0.4266	0.1032	0.1041	0.1076	0.1104	0.1140	0.1390
0.5065	0.1145	0.1171	0.1184	0.1208	0.1214	0.1464
0.5863	0.1272	0.1301	0.1294	0.1309	0.1312	0.1606
0.6661	0.1401	0.1435	0.1441	0.1453	0.1463	0.1727
0.7458	0.1560	0.1581	0.1575	0.1595	0.1590	0.1908
0.8254	0.1750	0.1787	0.1773	0.1788	0.1786	0.2056
0.9050	0.1946	0.1965	0.1960	0.1968	0.1969	0.2233
0.9845	0.2180	0.2177	0.2181	0.2184	0.2182	0.2495
1.0639	0.2411	0.2410	0.2420	0.2444	0.2410	0.2728
1.1431	0.2689	0.2705	0.2727	0.2705	0.2671	0.3021
1.2223	0.3016	0.3051	0.3046	0.3057	0.3037	0.3377
1.3014	0.3443	0.3455	0.3455	0.3456	0.3440	0.3790
1.3803	0.3961	0.3960	0.3955	0.3955	0.3975	0.4140
1.4591	0.4517	0.4541	0.4505	0.4550	0.4530	0.4853
1.5377	0.5340	0.5334	0.5303	0.5337	0.5310	0.5555
1.6162	0.6230	0.6276	0.6224	0.6254	0.6225	0.6371
1.6946	0.7393	0.7440	0.7395	0.7426	0.7417	0.7518
1.7728	0.8878	0.8867	0.8881	0.8938	0.8905	0.8945
1.8508	1.0540	1.0626	1.0642	1.0628	1.0591	1.0555
1.9286	1.2356	1.2539	1.2392	1.2381	1.2316	1.2129
2.0063	1.3720	1.3866	1.3752	1.3735	1.3621	1.3373
2.0837	1.3854	1.3948	1.3865	1.3895	1.3911	1.3656
2.1610	1.3418	1.3549	1.3460	1.3484	1.3523	1.3447
2.2380	1.2754	1.2625	1.2622	1.2743	1.2765	1.2681
2.3149	1.1984	1.1901	1.1797	1.1798	1.1930	1.1735
2.3915	1.1262	1.1173	1.1231	1.1175	1.1202	1.1070
2.4679	1.0760	1.0703	1.0719	1.0671	1.0775	1.0511
2.5440	1.0207	1.0198	1.0159	1.0218	1.0252	0.9940
2.6199	0.9876	0.9864	0.9864	0.9927	0.9796	0.9704
2.6956	0.9569	0.9549	0.9542	0.9519	0.9549	0.9533
2.7709	0.9576	0.9579	0.9576	0.9479	0.9494	0.9246
2.8461	0.9120	0.9125	0.9007	0.9109	0.9067	0.9051
2.9209	0.9177	0.9194	0.9187	0.9145	0.9096	0.9025
2.9955	0.9068	0.9026	0.9245	0.9138	0.9060	0.8964
3.0697	0.9045	0.8958	0.9036	0.9010	0.8994	0.8803
3.1437	0.9093	0.8955	0.9078	0.8959	0.9042	0.8721
3.2174	0.9165	0.9139	0.9007	0.9050	0.9033	0.8720
3.2907	0.9037	0.9153	0.9195	0.9135	0.9085	0.9055
3.3638	0.9335	0.9161	0.9283	0.9155	0.9225	0.8886
3.4365	0.9333	0.9347	0.9294	0.9282	0.9263	0.9103
3.5089	0.9447	0.9420	0.9319	0.9389	0.9234	0.9126

TABLE I. (*Continued*).

k \ T (K)	2.10	2.20	2.35	2.50	2.80	3.50
			$\rho = 150.29$ kg/m^3			
3.5810	0.9624	0.9752	0.9495	0.9666	0.9580	0.9496
3.6527	0.9791	0.9808	0.9810	0.9929	0.9698	0.9094
3.7240	0.9434	0.9386	0.9409	0.9354	0.9300	0.9441
3.7950	0.9702	0.9932	0.9591	0.9728	0.9549	1.0086
3.8656	0.9684	0.9784	0.9583	0.9518	0.9545	0.9708
3.9359	1.0130	1.0122	1.0097	1.0076	0.9850	1.0048
4.0058	0.9649	0.9935	0.9727	0.9651	0.9769	0.9308
4.0753	0.9595	0.9757	0.9819	0.9624	0.9766	0.9870
4.1444	0.9917	0.9811	0.9799	0.9954	0.9619	0.9122
4.2131	1.0007	1.0217	1.0209	1.0129	0.9878	1.0285
4.2814	0.9752	0.9812	0.9645	0.9898	0.9582	1.0100
4.3493	0.9821	0.9450	0.9541	0.9514	0.9522	0.9951
4.4167	0.9895	0.9828	1.0093	0.9877	0.9620	0.9922
4.4837	0.9602	0.9730	0.9736	0.9569	0.9399	0.9947
4.5504	1.0343	1.0822	1.0474	1.0625	1.0324	1.0334
4.6165	0.9853	0.9837	0.9479	0.9606	0.9635	0.9399
4.6822	0.9900	1.0018	0.9924	0.9681	0.9330	0.9556
4.7475	1.0173	1.0270	1.0051	1.0158	1.0220	0.9682
4.8123	1.0227	1.0496	1.0168	1.0184	1.0090	1.0109
4.8767	1.0125	0.9890	1.0302	1.0065	0.9848	1.0327
4.9406	0.9839	0.9923	0.9856	0.9890	0.9891	0.9664
5.0040	0.9941	0.9968	0.9807	0.9945	1.0068	1.0592
5.0669	1.0079	0.9916	1.0039	1.0151	1.0175	0.9463

k \ T (K)	1.16	1.30	1.40	1.50	1.60	1.80
			$\rho = 162.47$ kg/m^3			
0.1867	0.0612	0.0513	0.0639	0.0533	0.0667	0.0594
0.2667	0.0714	0.0641	0.0727	0.0640	0.0739	0.0697
0.3466	0.0850	0.0773	0.0868	0.0770	0.0874	0.0810
0.4266	0.0992	0.0913	0.0997	0.0898	0.0991	0.0941
0.5065	0.1126	0.1040	0.1144	0.1027	0.1138	0.1068
0.5863	0.1281	0.1168	0.1284	0.1155	0.1290	0.1187
0.6661	0.1440	0.1316	0.1455	0.1296	0.1447	0.1335
0.7458	0.1598	0.1457	0.1597	0.1448	0.1589	0.1490
0.8254	0.1771	0.1648	0.1787	0.1623	0.1784	0.1669
0.9050	0.1945	0.1822	0.1971	0.1758	0.1953	0.1842
0.9845	0.2208	0.2045	0.2224	0.2019	0.2201	0.2038
1.0639	0.2429	0.2205	0.2423	0.2237	0.2425	0.2255
1.1431	0.2708	0.2515	0.2718	0.2509	0.2706	0.2520
1.2223	0.3035	0.2845	0.3066	0.2813	0.3034	0.2832
1.3014	0.3402	0.3221	0.3418	0.3195	0.3431	0.3201
1.3803	0.3743	0.3679	0.3765	0.3622	0.3747	0.3645
1.4591	0.4403	0.4206	0.4396	0.4172	0.4383	0.4137
1.5377	0.5050	0.4955	0.5072	0.4885	0.5050	0.4878
1.6162	0.5824	0.5796	0.5870	0.5714	0.5810	0.5695
1.6946	0.6919	0.6899	0.6915	0.6778	0.6837	0.6720
1.7728	0.8271	0.8252	0.8283	0.8166	0.8255	0.8098
1.8508	0.9871	0.9906	0.9855	0.9807	0.9861	0.9824
1.9286	1.1771	1.1750	1.1807	1.1721	1.1836	1.1812
2.0063	1.3379	1.3475	1.3434	1.3485	1.3525	1.3717
2.0837	1.4019	1.4164	1.4078	1.4153	1.4196	1.4401
2.1610	1.3910	1.3998	1.3945	1.4047	1.3984	1.4198
2.2380	1.3184	1.3315	1.3200	1.3273	1.3216	1.3357
2.3149	1.2258	1.2408	1.2265	1.2082	1.2185	1.2347

TABLE I. (*Continued*).

k \ T (K)	1.16	1.30	1.40	1.50	1.60	1.80
			$\rho = 162.47$ kg/m^3			
2.3915	1.1535	1.1607	1.1498	1.1541	1.1410	1.1564
2.4679	1.0821	1.1008	1.0819	1.0929	1.0778	1.0956
2.5440	1.0229	1.0437	1.0214	1.0343	1.0172	1.0382
2.6199	0.9911	0.9992	0.9888	0.9984	0.9914	1.0003
2.6956	0.9618	0.9566	0.9571	0.9621	0.9694	0.9546
2.7709	0.9343	0.9551	0.9327	0.9497	0.9276	0.9573
2.8461	0.9119	0.9090	0.9037	0.9063	0.9184	0.9002
2.9209	0.9001	0.9020	0.8999	0.9057	0.8941	0.9053
2.9955	0.8946	0.9071	0.8955	0.9041	0.9000	0.9040
3.0697	0.8788	0.8870	0.8815	0.8859	0.8757	0.8927
3.1437	0.8582	0.8902	0.8681	0.8831	0.8636	0.8831
3.2174	0.8648	0.8927	0.8679	0.8858	0.8600	0.8953
3.2907	0.8889	0.8987	0.8844	0.8958	0.8929	0.9004
3.3638	0.8793	0.9090	0.8755	0.9002	0.8885	0.9132
3.4365	0.9017	0.9209	0.9052	0.9179	0.9011	0.9196
3.5089	0.9089	0.9216	0.9080	0.9190	0.9060	0.9289
3.5810	0.9404	0.9593	0.9347	0.9529	0.9483	0.9571
3.6527	0.9219	0.9592	0.9245	0.9527	0.9281	0.9732
3.7240	0.9539	0.9389	0.9698	0.9354	0.9699	0.9303
3.7950	1.0069	0.9696	1.0034	0.9722	1.0060	0.9627
3.8656	0.9597	0.9623	0.9585	0.9683	0.9735	0.9598
3.9359	1.0144	0.9982	1.0135	1.0020	1.0227	0.9967
4.0058	0.9234	0.9689	0.9363	0.9623	0.9353	0.9743
4.0753	0.9835	0.9696	0.9720	0.9723	0.9823	0.9617
4.1444	0.9398	0.9926	0.9347	0.9711	0.9457	0.9892
4.2131	1.0298	1.0026	1.0411	1.0035	1.0260	0.9946
4.2814	0.9999	0.9743	1.0197	0.9840	1.0246	0.9860
4.3493	0.9858	0.9548	1.0111	0.9610	0.9931	0.9496
4.4167	0.9887	0.9852	0.9775	0.9777	0.9914	1.0052
4.4837	0.9960	0.9583	0.9919	0.9832	1.0103	0.9798
4.5504	1.0228	1.0358	1.0110	1.0333	1.0524	1.0436
4.6165	0.9444	0.9711	0.9664	0.9630	0.9780	0.9893
4.6822	0.9814	0.9879	0.9897	0.9869	0.9830	0.9883
4.7475	0.9632	1.0121	0.9673	1.0017	0.9778	0.9853
4.8123	0.9883	1.0147	0.9943	1.0074	1.0014	1.0138
4.8767	1.0400	1.0196	1.0301	1.0139	1.0359	1.0086
4.9406	0.9654	0.9776	1.0001	0.9915	0.9592	0.9707
5.0040	1.0257	0.9875	1.0131	0.9911	1.0089	0.9943
5.0669	0.9995	0.9977	0.9803	1.0001	1.0133	1.0099

k \ T (K)	2.00	2.10	2.30	2.50	2.80
			$\rho = 162.47$ kg/m^3		
0.1867	0.0640	0.0668	0.0635	0.0674	0.0721
0.2667	0.0706	0.0721	0.0677	0.0721	0.0769
0.3466	0.0818	0.0838	0.0769	0.0810	0.0850
0.4266	0.0931	0.0939	0.0880	0.0901	0.0944
0.5065	0.1051	0.1062	0.0989	0.1019	0.1029
0.5863	0.1170	0.1163	0.1105	0.1131	0.1150
0.6661	0.1309	0.1321	0.1225	0.1261	0.1284
0.7458	0.1448	0.1449	0.1364	0.1385	0.1410
0.8254	0.1634	0.1632	0.1532	0.1565	0.1575
0.9050	0.1804	0.1814	0.1712	0.1732	0.1756
0.9845	0.2009	0.2003	0.1918	0.1929	0.1946

TABLE I. (*Continued*).

k \ T (K)	2.00	2.10	2.30	2.50	2.80
			$\rho=162.47$ kg/m^3		
1.0639	0.2225	0.2230	0.2114	0.2137	0.2183
1.1431	0.2483	0.2494	0.2374	0.2391	0.2408
1.2223	0.2786	0.2770	0.2682	0.2698	0.2704
1.3014	0.3154	0.3164	0.3035	0.3061	0.3105
1.3803	0.3591	0.3580	0.3464	0.3499	0.3530
1.4591	0.4088	0.4113	0.3956	0.4007	0.4039
1.5377	0.4787	0.4829	0.4650	0.4709	0.4717
1.6162	0.5609	0.5608	0.5473	0.5518	0.5547
1.6946	0.6633	0.6653	0.6554	0.6527	0.6573
1.7728	0.7980	0.7988	0.7860	0.7878	0.7953
1.8508	0.9707	0.9733	0.9591	0.9595	0.9666
1.9286	1.1794	1.1829	1.1720	1.1705	1.1746
2.0063	1.3850	1.4024	1.3826	1.3863	1.3891
2.0837	1.4684	1.4930	1.4806	1.4791	1.4819
2.1610	1.4403	1.4425	1.4465	1.4594	1.4577
2.2380	1.3419	1.3474	1.3379	1.3538	1.3740
2.3149	1.2326	1.2284	1.2271	1.2442	1.2538
2.3915	1.1482	1.1404	1.1415	1.1468	1.1601
2.4679	1.0860	1.0798	1.0828	1.0886	1.0971
2.5440	1.0233	1.0202	1.0172	1.0233	1.0326
2.6199	0.9871	0.9775	0.9841	0.9858	0.9950
2.6956	0.9502	0.9489	0.9383	0.9550	0.9626
2.7709	0.9482	0.9398	0.9372	0.9482	0.9506
2.8461	0.8991	0.8927	0.8874	0.8861	0.9040
2.9209	0.8976	0.9071	0.8977	0.8960	0.9129
2.9955	0.8987	0.8978	0.8970	0.8965	0.9020
3.0697	0.8855	0.8821	0.8796	0.8923	0.8970
3.1437	0.8872	0.8876	0.8852	0.8856	0.8839
3.2174	0.8893	0.8981	0.8807	0.8999	0.9031
3.2907	0.8987	0.8896	0.8793	0.8953	0.9008
3.3638	0.9052	0.9050	0.9041	0.9056	0.9083
3.4365	0.9321	0.9289	0.9278	0.9221	0.9376
3.5089	0.9274	0.9239	0.9193	0.9283	0.9204
3.5810	0.9543	0.9588	0.9592	0.9679	0.9775
3.6527	0.9704	0.9770	0.9728	0.9703	0.9730
3.7240	0.9354	0.9297	0.9311	0.9353	0.9460
3.7950	0.9750	0.9534	0.9429	0.9737	0.9642
3.8656	0.9716	0.9761	0.9494	0.9661	0.9800
3.9359	1.0007	0.9883	0.9876	0.9836	1.0042
4.0058	0.9719	0.9887	0.9827	0.9712	1.0011
4.0753	0.9762	0.9650	0.9617	0.9714	0.9590
4.1444	0.9945	0.9896	0.9758	0.9754	0.9621
4.2131	1.0175	1.0097	0.9946	0.9958	0.9843
4.2814	0.9925	0.9894	0.9470	0.9635	0.9791
4.3493	0.9764	0.9599	0.9200	0.9599	0.9642
4.4167	0.9912	1.0054	0.9777	0.9670	1.0046
4.4837	0.9675	0.9694	0.9597	0.9711	0.9670
4.5504	1.0473	1.0510	1.0419	1.0476	1.0639
4.6165	0.9846	0.9686	0.9647	0.9660	0.9786
4.6822	0.9671	0.9658	0.9862	0.9817	0.9918
4.7475	1.0223	0.9945	0.9604	1.0139	0.9775
4.8123	1.0284	0.9811	1.0263	1.0373	0.9978
4.8767	1.0066	0.9864	0.9897	0.9941	1.0000
4.9406	0.9890	1.0293	0.9954	0.9882	0.9939
5.0040	0.9839	0.9754	0.9915	0.9936	0.9875
5.0669	1.0121	1.0370	1.0069	1.0013	1.0327

TABLE I. (*Continued*).

k \ T (K)	1.16	1.30	1.40	1.50	1.60	1.75
			$\rho = 171.00$ kg/m^3			
0.1867	0.0554	0.0447	0.0485	0.0472	0.0601	0.0442
0.2667	0.0648	0.0553	0.0657	0.0569	0.0669	0.0553
0.3466	0.0777	0.0660	0.0782	0.0683	0.0790	0.0646
0.4266	0.0905	0.0776	0.0916	0.0805	0.0912	0.0763
0.5065	0.1030	0.0888	0.1051	0.0913	0.1040	0.0866
0.5863	0.1169	0.1015	0.1188	0.1023	0.1185	0.0982
0.6661	0.1312	0.1130	0.1327	0.1157	0.1323	0.1108
0.7458	0.1472	0.1269	0.1480	0.1290	0.1479	0.1236
0.8254	0.1626	0.1442	0.1654	0.1460	0.1639	0.1390
0.9050	0.1799	0.1598	0.1817	0.1621	0.1804	0.1510
0.9845	0.2043	0.1796	0.2039	0.1813	0.2044	0.1705
1.0639	0.2237	0.1991	0.2242	0.2013	0.2236	0.1900
1.1431	0.2505	0.2230	0.2523	0.2249	0.2511	0.2139
1.2223	0.2797	0.2522	0.2823	0.2553	0.2801	0.2380
1.3014	0.3141	0.2871	0.3160	0.2897	0.3149	0.2704
1.3803	0.3440	0.3311	0.3459	0.3315	0.3459	0.3128
1.4591	0.4019	0.3780	0.4031	0.3767	0.4027	0.3588
1.5377	0.4650	0.4435	0.4658	0.4480	0.4635	0.4207
1.6162	0.5329	0.5274	0.5349	0.5202	0.5325	0.4965
1.6946	0.6306	0.6213	0.6321	0.6189	0.6311	0.5942
1.7728	0.7611	0.7460	0.7605	0.7444	0.7592	0.7153
1.8508	0.9164	0.9071	0.9137	0.9085	0.9131	0.8690
1.9286	1.1135	1.1094	1.1194	1.1046	1.1244	1.0748
2.0063	1.3209	1.3260	1.3311	1.3289	1.3441	1.3247
2.0837	1.4471	1.4550	1.4526	1.4592	1.4750	1.4854
2.1610	1.4646	1.4864	1.4690	1.4745	1.4821	1.5079
2.2380	1.3826	1.4113	1.3900	1.3891	1.3906	1.4165
2.3149	1.2712	1.3040	1.2702	1.2776	1.2693	1.2929
2.3915	1.1778	1.2079	1.1769	1.1805	1.1731	1.1886
2.4679	1.0980	1.1325	1.1015	1.1098	1.0989	1.1187
2.5440	1.0311	1.0633	1.0354	1.0437	1.0356	1.0347
2.6199	0.9923	1.0142	0.9995	0.9941	0.9911	1.0003
2.6956	0.9647	0.9661	0.9667	0.9529	0.9611	0.9545
2.7709	0.9295	0.9585	0.9248	0.9455	0.9356	0.9409
2.8461	0.9021	0.9074	0.9037	0.8917	0.9064	0.8883
2.9209	0.9001	0.9085	0.8894	0.8905	0.9007	0.8981
2.9955	0.8883	0.8967	0.8908	0.8955	0.8888	0.8978
3.0697	0.8657	0.8777	0.8672	0.8714	0.8659	0.8813
3.1437	0.8539	0.8911	0.8558	0.8663	0.8597	0.8699
3.2174	0.8471	0.8859	0.8446	0.8772	0.8587	0.8825
3.2907	0.8792	0.8880	0.8890	0.8816	0.8826	0.8932
3.3638	0.8749	0.8939	0.8806	0.8958	0.8754	0.8947
3.4365	0.8933	0.9075	0.8918	0.9076	0.8919	0.9137
3.5089	0.8920	0.9214	0.8873	0.9181	0.8926	0.9147
3.5810	0.9258	0.9515	0.9317	0.9424	0.9165	0.9427
3.6527	0.9189	0.9510	0.9208	0.9569	0.9189	0.9603
3.7240	0.9540	0.9259	0.9685	0.9143	0.9692	0.9271
3.7950	1.0007	0.9554	0.9922	0.9479	1.0133	0.9583
3.8656	0.9747	0.9528	0.9694	0.9495	0.9714	0.9547
3.9359	1.0071	0.9877	1.0141	0.9878	1.0051	0.9804
4.0058	0.9286	0.9544	0.9263	0.9677	0.9193	0.9862
4.0753	0.9944	0.9628	0.9837	0.9554	0.9999	0.9679
4.1444	0.9315	0.9835	0.9296	0.9587	0.9545	0.9660
4.2131	1.0294	0.9851	1.0155	0.9898	1.0349	0.9986
4.2814	1.0097	0.9780	1.0217	0.9640	1.0231	0.9437
4.3493	0.9857	0.9449	0.9669	0.9480	1.0030	0.9625
4.4167	0.9703	0.9885	0.9817	0.9773	0.9770	0.9834

TABLE I. (*Continued*).

k \ T (K)	1.16	1.30	1.40	1.50	1.60	1.75
			$\rho=171.00$ kg/m^3			
4.4837	0.9942	0.9863	0.9835	0.9694	0.9852	0.9363
4.5504	1.0228	1.0445	1.0296	1.0354	1.0180	1.0392
4.6165	0.9688	0.9732	0.9693	0.9837	0.9492	0.9654
4.6822	0.9920	0.9644	0.9845	0.9675	1.0161	0.9684
4.7475	0.9734	0.9912	0.9678	1.0097	0.9691	1.0245
4.8123	1.0049	1.0298	1.0003	0.9957	1.0142	1.0114
4.8767	1.0450	1.0129	1.0436	1.0222	1.0373	1.0253
4.9406	0.9427	0.9833	0.9600	0.9867	0.9728	0.9898
5.0040	1.0206	0.9869	1.0275	0.9961	1.0176	0.9774
5.0669	0.9990	1.0027	0.9829	1.0138	0.9686	1.0081
k \ T (K)	1.85	1.90	2.10	2.30	2.50	2.80
			$\rho=171.00$ kg/m^3			
0.1867	0.0541	0.0480	0.0511	0.0535	0.0555	0.0613
0.2667	0.0625	0.0555	0.0583	0.0597	0.0620	0.0659
0.3466	0.0725	0.0648	0.0676	0.0689	0.0698	0.0736
0.4266	0.0852	0.0763	0.0787	0.0796	0.0810	0.0846
0.5065	0.0963	0.0865	0.0894	0.0898	0.0908	0.0933
0.5863	0.1068	0.0972	0.0995	0.1001	0.1012	0.1039
0.6661	0.1202	0.1103	0.1114	0.1115	0.1132	0.1159
0.7458	0.1334	0.1225	0.1244	0.1251	0.1264	0.1288
0.8254	0.1510	0.1389	0.1419	0.1417	0.1427	0.1466
0.9050	0.1660	0.1546	0.1566	0.1571	0.1587	0.1600
0.9845	0.1854	0.1721	0.1755	0.1758	0.1765	0.1804
1.0639	0.2057	0.1944	0.1947	0.1967	0.1954	0.1992
1.1431	0.2314	0.2155	0.2172	0.2186	0.2181	0.2226
1.2223	0.2600	0.2459	0.2453	0.2469	0.2465	0.2477
1.3014	0.2948	0.2761	0.2798	0.2785	0.2815	0.2857
1.3803	0.3344	0.3157	0.3186	0.3202	0.3218	0.3254
1.4591	0.3823	0.3645	0.3643	0.3656	0.3680	0.3688
1.5377	0.4483	0.4268	0.4316	0.4308	0.4347	0.4345
1.6162	0.5213	0.4978	0.5010	0.5029	0.5052	0.5070
1.6946	0.6171	0.5970	0.5962	0.5979	0.6008	0.6017
1.7728	0.7387	0.7204	0.7171	0.7207	0.7230	0.7232
1.8508	0.8999	0.8832	0.8849	0.8818	0.8857	0.8910
1.9286	1.1113	1.0921	1.1084	1.0999	1.1044	1.0941
2.0063	1.3598	1.3611	1.3726	1.3647	1.3623	1.3533
2.0837	1.5197	1.5262	1.5433	1.5454	1.5420	1.5294
2.1610	1.5304	1.5316	1.5509	1.5573	1.5603	1.5542
2.2380	1.4222	1.4222	1.4286	1.4399	1.4449	1.4447
2.3149	1.2957	1.2858	1.2873	1.2941	1.3023	1.3125
2.3915	1.1754	1.1755	1.1741	1.1859	1.1850	1.1901
2.4679	1.1031	1.1020	1.1006	1.1092	1.1126	1.1202
2.5440	1.0402	1.0398	1.0313	1.0342	1.0430	1.0448
2.6199	1.0010	0.9821	0.9893	0.9884	0.9897	0.9936
2.6956	0.9513	0.9444	0.9506	0.9510	0.9526	0.9628
2.7709	0.9537	0.9357	0.9412	0.9471	0.9478	0.9491
2.8461	0.9035	0.8897	0.8863	0.8845	0.8951	0.8974
2.9209	0.9016	0.8860	0.8963	0.9025	0.8980	0.9027
2.9955	0.8977	0.8853	0.8953	0.8912	0.8943	0.9027
3.0697	0.8732	0.8834	0.8774	0.8713	0.8832	0.8729
3.1437	0.8838	0.8727	0.8793	0.8730	0.8836	0.8874

TABLE I. (*Continued*).

k	T (K) 1.85	1.90	2.10	2.30	2.50	2.80
			$\rho=171.00$ kg/m^3			
3.2174	0.8799	0.8744	0.8848	0.8833	0.8888	0.8938
3.2907	0.8884	0.8734	0.8924	0.8854	0.8880	0.8844
3.3638	0.9031	0.8979	0.9059	0.9017	0.8979	0.9037
3.4365	0.9221	0.9122	0.9270	0.9151	0.9234	0.9222
3.5089	0.9242	0.9162	0.9211	0.9163	0.9273	0.9323
3.5810	0.9493	0.9268	0.9578	0.9478	0.9602	0.9477
3.6527	0.9723	0.9644	0.9693	0.9629	0.9625	0.9751
3.7240	0.9355	0.9235	0.9254	0.9205	0.9426	0.9457
3.7950	0.9533	0.9465	0.9691	0.9559	0.9660	0.9610
3.8656	0.9616	0.9596	0.9551	0.9571	0.9570	0.9745
3.9359	1.0032	0.9764	1.0017	0.9962	1.0100	1.0048
4.0058	0.9974	0.9658	0.9726	0.9752	0.9948	0.9819
4.0753	0.9765	0.9609	0.9616	0.9626	0.9748	0.9649
4.1444	0.9874	0.9744	0.9888	0.9833	0.9852	0.9987
4.2131	1.0168	0.9930	0.9965	1.0028	1.0196	1.0081
4.2814	0.9746	0.9683	0.9764	0.9781	0.9896	0.9717
4.3493	0.9770	0.9704	0.9627	0.9599	0.9630	0.9727
4.4167	1.0066	0.9778	0.9615	0.9800	1.0003	0.9778
4.4837	0.9759	0.9560	0.9603	0.9551	0.9971	0.9793
4.5504	1.0374	1.0152	1.0461	1.0399	1.0652	1.0207
4.6165	0.9910	0.9688	0.9722	0.9702	0.9701	0.9625
4.6822	0.9731	0.9690	0.9692	0.9616	0.9965	0.9880
4.7475	0.9960	1.0027	1.0170	1.0056	1.0010	1.0148
4.8123	1.0069	1.0481	1.0242	1.0128	1.0153	1.0012
4.8767	1.0228	0.9898	1.0113	1.0002	1.0221	1.0144
4.9406	0.9890	0.9732	0.9883	0.9852	1.0021	1.0018
5.0040	0.9959	0.9960	0.9790	0.9816	0.9667	0.9849
5.0669	1.0052	0.9990	1.0037	1.0168	1.0086	1.0227

of the roton minimum ~ 0.1 Å^{-1} below the maximum in $S(k)$. Our data show a similar behavior (Fig. 4) with the amplitude of the effect being ~ 0.025 Å^{-1}.

GMR's theory provides good semiquantitative predictions for the behavior of $S(k)$ and it provides rather surprising quantitative agreement with our results for the behavior of the peak in $S(k)$ over the entire range of density and temperature where validity of the theory is claimed. In addition, it gives us a basis for understanding the cause of the apparent continuation of the anomalous behavior of $S(k)$ above T_λ, especially at high density.

V. THE PAIR-CORRELATION FUNCTION AND THE CONDENSATE FRACTION

The pair correlation function $g(r)$ can be directly calculated from $S(k)$ by the Fourier transform,

$$g(r)=\left[\frac{1}{2\pi^2\rho r}\int k\sin(kr)[S(k)-1]dk\right]+1\ . \qquad (5)$$

This integral was applied to the data and performed numerically on 1000 smoothed structure factor data points in the range of k for which we have data and for 120 values of r at each temperature and density measured. Values for the pair-correlation function deduced from the $S(k)$ values we report here are available[25] from the AIP Physics Auxiliary Publication Service. A typical $g(r)$ is shown in Fig. 7. Note that for $r\leq 2$ Å the results become unreliable due to the finite-momentum-transfer range of our data. The spurious oscillations seen for $r\leq 2$ Å are much smaller in amplitude than those encountered in earlier work here.[3,4]

In 1970, Hyland, Rowlands, and Cummings[26] (HRC) proposed a method for determining the condensate fraction in superfluid helium from its measured pair-correlation function. It should be pointed out that while this alternative microscopic approach to the explanation of the changes in spatial order with temperature in He II is not *a priori* in conflict with the microscopic theories of GMR, the survival of rotons above T_λ makes a reconciliation of the two points of view very unlikely.

An intuitive picture of the (HRC) proposal is appealing: Below T_λ a finite occupation condensate fraction of zero momentum exists. To the extent that an atom participates in the condensate, it becomes spatially delocalized. Thus, HRC suggest a picture in which a background of uniform density forms at the expense of the usual spatial structure of the helium. The signature of this phenomena would be a decrease in the height of the peaks of $S(k)$ and $g(r)$ with their locations remaining unchanged. This is,

in fact, what is observed[5,6] except for the small motion of the peak in $S(k)$ reported earlier.

On the basis of their model, HRC calculate an expression for n_0, the condensate fraction. Beginning with a factorization of the reduced density matrix first suggested by Penrose,[23] they proceed to the limit of $r > r_0 \simeq 4.5$ Å and find an expression, following Frohlich,[27] for the equilibrium pair-correlation function. They derive an expression for the condensate fraction $n_0(T)$ in terms of the radial distribution function $g(r,T)$ at the temperature, T, of interest and a function $g(r,T^*)$ which they identify as the pair-correlation function either just above T_λ or that function extrapolated to the temperature under consideration. The derived expression is

$$n_0(T) = 1 - \left[\frac{g(r,T)-1}{g(r,T^*)-1} \right]^{1/2} . \quad (6)$$

It should be noted that this theory is not without its critics. Fetter[28] provides as a counterexample, a weakly interacting Bose gas at low temperature which undergoes Bose condensation and satisfies the various criteria put forward by HRC but which fails to obey Eq. (6). Chester and Reatto[29] criticize the theoretical basis of Eq. (6) in two ways. They point out that identifying $g(r,T^*)$ with the radial distribution function at T^* just above T_λ is an assumption unjustified by the theoretical development. Further, they suggest that the power to which the quotient is raised in Eq. (6) is arbitrary, HRC's proof being amenable to modification of this exponent by any constant factor. Griffin[30] indicates that when the analysis of Fröhlich is generalized to include both diagonal and off-diagonal density matrix terms, (the so-called "anomalous terms") HRC's assumptions in the limit of $r \geq 4.5$ Å are no longer true. In particular, they calculate the one-phonon contribution to $g(r)$ and find it non-negligible throughout the range $4.5 < 4 < 12$ Å considered by HRC. HRC have replied to this criticism[31] indicating that the so-called anomalous terms had been correctly incorporated in their theory in the form of screening factors for the hard core repulsive potentials. They indicate that their identification of $g(r,T^*)$ as the radial distribution function at $T = T_\lambda$ *is* an assumption and has yet to be justified microscopically. They criticize Fetter's counterexample

TABLE II. Parameters determined from fits to the experimentally determined liquid-structure values. Here S_M is the height of the principal structure factor peak, k_M is the location of S_M in momentum transfer, Δ_M is the maximum of the quantity $[S(k,T,\rho)-S(k,1.16\text{ K},\rho)]$ at the relevant density, and k_Δ is the location of Δ_M in momentum transfer.

T (K)	S_M	K_M	Δ_M	k_Δ
		$\rho = 150.29$ kg/m^3		
1.1600	1.3394	2.0644	0.0000	3.0000
1.3000	1.3395	2.0644	0.0101	2.5450
1.4000	1.3340	2.0644	−0.0028	1.9500
1.6000	1.3453	2.0696	0.0093	2.4350
1.7500	1.3573	2.0696	0.0184	2.0850
1.9000	1.3840	2.0696	0.0459	2.0950
2.1000	1.3907	2.0592	0.0519	2.0450
2.2000	1.4051	2.0592	0.0658	2.0550
2.3500	1.3946	2.0592	0.0553	2.0550
2.5000	1.3941	2.0592	0.0548	2.0550
2.8000	1.3928	2.0748	0.0549	2.0950
3.5000	1.3704	2.0852	0.0367	2.1250
		$\rho = 162.47$ kg/m^3		
1.1600	1.4067	2.1060	0.0000	3.0000
1.3000	1.4195	2.1060	0.0130	2.0800
1.4000	1.4751	2.1320	0.0110	1.9850
1.5000	1.4821	2.1320	0.0122	2.0800
1.6000	1.4940	2.1268	0.0271	2.0600
1.7500	1.5158	2.1320	0.0450	2.1450
1.8500	1.5443	2.1268	0.0742	2.1100
1.9000	1.5481	2.1268	0.0787	2.1050
2.1000	1.5680	2.1268	0.0984	2.1100
2.3000	1.5730	2.1268	0.1024	2.1200
2.5000	1.5732	2.1320	0.1022	2.1300
2.8000	1.5637	2.1320	0.0926	2.1350
		$\rho = 171.0$ kg/m^3		
1.1600	1.4711	2.1320	0.0000	3.0000
1.3000	1.4874	2.1372	0.0296	2.2500
1.4000	1.4751	2.1320	0.0110	1.9850
1.5000	1.4821	2.1320	0.0122	2.0800
1.6000	1.4940	2.1268	0.0271	2.0600
1.7500	1.5158	2.1320	0.0450	2.1450
1.8500	1.5443	2.1268	0.0742	2.1100
1.9000	1.5481	2.1268	0.0787	2.1050
2.1000	1.5680	2.1268	0.0984	2.1100
2.3000	1.5730	2.1268	0.1024	2.1200
2.5000	1.5732	2.1320	0.1022	2.1300
2.8000	1.5637	2.1320	0.0926	2.1350

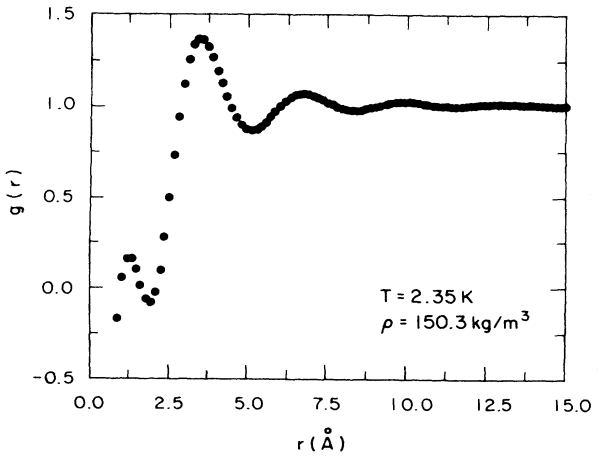

FIG. 7. A typical radial distribution function ($T = 2.35$ K, $\rho = 150.29$ kg/m^3) calculated by numerical integration of fitted $S(k)$ values. The structure at small r ($r \leq 2.5$ Å) results from uncertainties in our large k $S(k)$'s.

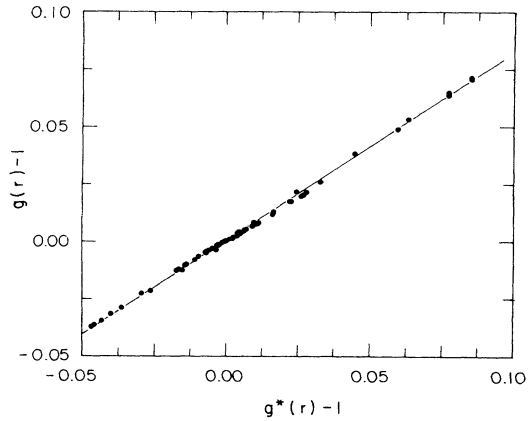

FIG. 8. A typical determination of n_0 by this means. Data points between $r=5.85$ and 14.1 Å are shown as well as the least-squares straight line fit. For these data at $T=1.16$ K, $\rho=171$ kg/m^3, the slope is $s=0.81$, and $n_0=1-\sqrt{s}=0.10$. The reference g^* is taken at $T=2.2$ K, $\rho=171$ kg/m^3.

as being of doubtful relevance to real ^{4}He and further justify some of their assumptions on the basis of work by McMillan[32] and Yukalov.[33] Obviously the use of Eq. (6) to extract values of n_0 is somewhat questionable and our point of view remains[5] that the validity of the prescription [Eq. (6)] has yet to be firmly established.

In spite of this caveat, it is of interest to apply Eq. (6) to the data. We choose[5] to calculate n_0 by plotting $g(r,T)-1$ versus $g(r,T^*)-1$ for $r\gtrsim 4.5$ Å and then define $n_0=1-S^{1/2}$, where S is the slope of the resulting straight line fit to the data. An example of such a plot along with the straight line is shown in Fig. 8. As is readily seen from Fig. 8 there is an excellent linear relationship. In general, a determination of n_0 from the data by this technique is straightforward. For the data at the highest density, however, the greatest structure is not observed just above T_λ, but at a somewhat higher temperature. In this case the choice of the particular data set for T^* can make a change of ~ 0.002 in the computed value for n_0. We regard this as a possible systematic error which does not affect any of our conclusions. Values of n_0 determined from the data are shown in Fig. 9 as a function of T/T_λ and presented in Table III. We have calculated values for each $g(r)$ rather than presenting averages to give a better picture of the scatter in the results. At the lowest density (which is close to saturated vapor pressure) the results of the application of Eq. (6) to the data are in excellent agreement with similar determinations at saturated vapor pressure made by neutron scattering techniques. The fact that there is little apparent dependence of n_0 on density as T is reduced is contrary to predictions[34] that this value should vary from $\gtrsim 10\%$ at saturated vapor pressure to a few percent near the solidification point ($\rho\sim 172$ kg/m^3).

Recently, inelastic neutron scattering techniques have been used to study[35,36] the condensate fraction question in response to the suggestion by Hohenburg and Platzman that such techniques may offer a more direct measurement. Results as a function of density at $T=1.0$ K by Sokol *et al.*[37] show the condensate fraction to decrease with an increase in density; the dependence is weaker than expected theoretically but stronger than given by the HRC prescription applied to our data.

We fit each of these sets of data to the function $n_0=A[1-(T/T_\lambda)^B]$ which is the expected temperature dependence of the condensate fraction for an ideal Bose-Einstein gas. While there is little theoretical justification

TABLE III. Values of the quantity $n_0(T,\rho)$ determined by the method due to Hyland *et al.* (Ref. 25), $n_0(1)$'s; due to Sears (Ref. 38), $n_0(2)$'s.

	$\rho=150.29$ kg/m^3		$\rho=162.47$ kg/m^3		$\rho=171.00$ kg/m^3	
I	$n_0(1)$	$n_0(2)$	$n_0(1)$	$n_0(2)$	$n_0(1)$	$n_0(2)$
1.16	0.101	0.146	0.101	0.151	0.103	0.153
1.16	0.102	0.152	0.104	0.109	0.103	0.096
1.30	0.109	0.159	0.092	0.144	0.092	0.135
1.30	0.104	0.151	0.100	0.123	0.097	0.141
1.30	0.098	0.130	0.093	0.146		
1.40	0.101	0.136	0.097	0.108	0.095	0.129
1.50			0.086	0.140	0.091	0.140
1.50					0.083	0.127
1.60	0.092	0.117	0.084	0.088	0.079	0.102
1.60	0.087	0.132				
1.75	0.073	0.082			0.041	0.098
1.80			0.059	0.111		
1.80			0.056	0.084		
1.85					0.030	0.062
1.90	0.043	0.096			0.014	0.033
2.00			0.017	0.038		
2.00			0.019	0.052		
2.10	0.018	0.045				

TABLE IV. Parameters A and B obtained by fitting $n_0=A[1-(T/T_\lambda)^B]$ to the n_0 values deduced from Eq. (6).

ρ (kg/m^3)	150.29	162.47	171.00
A	0.1085±0.0034	0.1031±0.1027	0.1067±0.0034
B	5.38 ±0.59	5.78 ±0.48	6.23 ±0.63

for the use of this form for interacting liquid helium, it fits the data well and provides a uniform methodology for obtaining values of $n_0(T=0\text{ K})$, i.e., A. For the cases in question we have used T_λ $(\rho=150.29)=2.15$ K, T_λ $(\rho=162.47)=2.05$ K, and T_λ $(\rho=171.0)=1.938$ K. The results of fits to the data are tabulated in Table IV. If all the data are fit to a single curve we find $A=0.105\pm0.002$; $B=5.71\pm0.33$.

Thus both A and B (and hence n_0) appear to be nearly independent of density in the range considered in this work. This result suggests either that the condensate fraction has surprisingly little density dependence or that Eq. (6) really is inappropriate for the extraction of condensate fraction values.

Another possibility for determining the condensate fraction from $g(r)$ was suggested by Sears.[38] The potential energy of a helium atom can be calculated from the cluster expansion $V=V_2+V_3+\cdots$ with

$$V_2=2\pi\rho\int_0^\infty \phi(r)g(r)r^2dr\ .$$

The total energy per atom U can be derived from thermodynamic measurements. The difference $K=U-V$ is the kinetic energy per atom. Below T_λ we can express $K=(1-n_0)K^*$, where K^* is the average kinetic energy of atoms not in the condensate. If we then assume K^* is not a strong function of T and that $K^*(T)\simeq K(T_\lambda)$ we arrive at an approximate expression for n_0:

$$n_0=1-\frac{K(T)}{K(T_0)}\ . \tag{7}$$

We have interpolated values for U from thermodynamic tables of Maynard[17] below T_λ and from those of McCarty[39] above T_λ. Values of V_2 were calculated using our experimental $g(r)$'s and the Hartree-Fock dispersion (HFDHE2) potential, $\phi(r)$ of Aziz *et al.*[40] Values of V_3 were interpolated from the results of Kalos *et al.*[41] derived from this same potential. The results are displayed in Table III and Fig. 9. The uncertainties in this set of calculations are difficult to estimate. The random error generated by our experimental data was 10% in n_0. Our thermodynamic values agree in their region of overlap by about 8%. This uncertainty is reflected in variations of n_0 of ±0.01. An overall uncertainty in n_0 of ±0.015 seems reasonable. As can be seen, although n_0's calculated by this method are systematically higher than the HRC values, there is, again, little discernable pressure dependence. We have fitted these alternate values for n_0 to the function $n_0=a[1-(T/T_\lambda)^b]$ with the result that $a=n_0(T=0)=0.119\pm0.003$ with an exponent b of 9.9 ± 1.3.

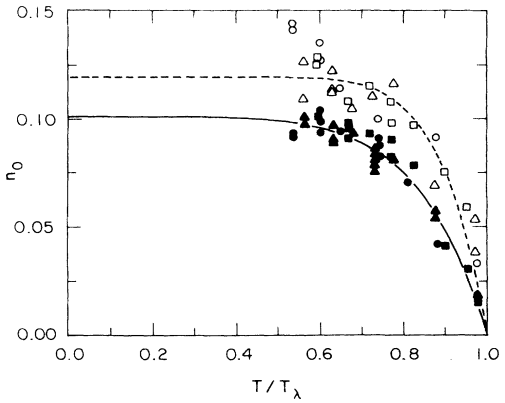

FIG. 9. n_0 vs T/T_λ as determined by the two techniques described in the text [Hyland *et al.* (Ref. 25) (solid symbols), Eq. (6); Sears (Ref. 38) (open symbols), Eq. (7)] for the three density values: (●) 150.29, (▲) 167.47, and (■) 171.0 kg/m^3. For each technique the results are fit to the functional form $n_0=A[1-(T/T_\lambda)^B]$; the curve is the fit in each case.

Sears also proposes[38] three other methods for the determination of n_0 from the dynamic structure factor $S(k,\omega)$ and the total scattering cross section $\sigma(E_0)$. Values of the condensate fraction are reported by Sears at saturated vapor pressure (SVP) by most of these methods. Within their respective errors, there are no significant differences between our higher density results and those reported by Sears at SVP.

This apparent lack of sensitivity in the value of n_0 to changes in density must be considered a problem indicative of either serious difficulties with the correctness of Eq. (6) or of our understanding of how the condensate fraction must behave with changes in density. It has been assumed that at increased density the stronger interactions among the atoms would deplete the condensate. If Eq. (6) has validity (as comparisons between its results and those of high-energy inelastic neutron[36] experiments at saturated vapor pressure seem to suggest) then our understanding of the depletion of the condensate is incomplete. Another possibility is that Eq. (6) is essentially valid at saturated vapor pressure but not at higher values of the density; this seems unlikely.

VI. COMPARISON TO EARLIER WORK

We next compare data from the present experiment with earlier data obtained[3,4] as a function of density in this laboratory. Those earlier data[3,4] were reduced from the raw scattering count rates by a procedure different from that used here. For consistency and to remove the recently discovered anomaly in the EPC normalization, the earlier data were reanalyzed without the intensity scale factors generated by the EPC. The result was a very con-

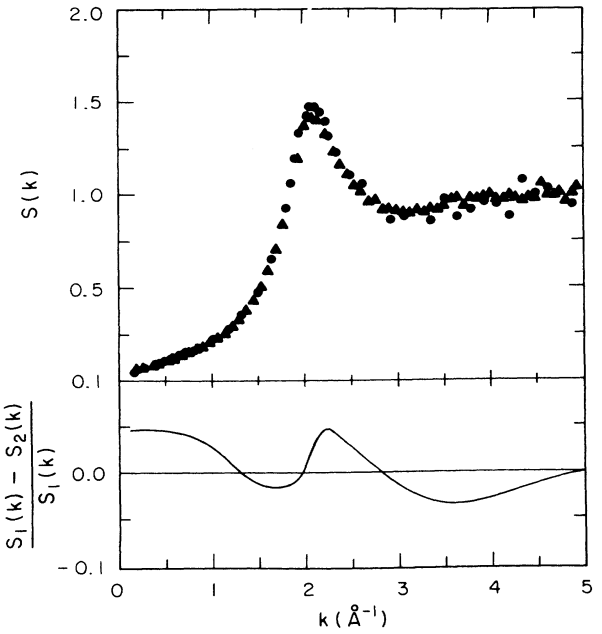

FIG. 10. A typical comparison of previous data by Robkoff and Hallock (Refs. 3 and 4) (●) with new data (▲) at $T=1.67$ K and 10 atm pressure. Data have been shifted in relative angle by 6.9×10^{-3} rad to compensate for incident beam shifts. Lower plot is the fractional difference between these data.

sistent lowering of the principal peak in the structure factor by about 5%, due mainly to changes in the neon and empty cell scans. We believe these recalculated values for $S(k)$ and $g(r)$, reported in Ref. 25 have now eliminated an important source of systematic error. It should be noted, however, that the elimination of the EPC correction has also made $S(k)$ sensitive to variations in x-ray intensity during a scan. Since these early data scans were done with an anode that degraded much more rapidly than the anode used for the presently reported data, an uncontrolled variable exists that probably accounts for the internal consistency of ~2% in the measured peak height of a fiducial scan which was repeated several times during that experiment. The original estimate of an absolute error of ~4% is still appropriate.

In order to facilitate a comparison of the recalculated $S(k)$'s with our newly reported data, we reproduced temperature and density values from the old data in the course of these new runs. We have calculated the percent deviation between the two fitted structure factors as a function of k and present the results in Fig. 10. As can be seen, our values agree to within a few percent everywhere.

Values of these[3,4] data as reanalyzed are available[25] in the form of tables of experimentally determined structure factor values and tables of fitted and smoothed $S(k)$ values.

VII. SUMMARY AND CONCLUSION

We have measured the structure factor of liquid ^{4}He by x-ray scattering at three densities in the temperature range $1.16\leq T\leq 3.5$ K. The anomalous behavior of $S(k)$ at and below T_λ agrees well with predictions by Reatto *et al.*,[22] which calculate the effect of thermally populated roton states on the liquid structure. Two different methods proposed for extracting the condensate fraction n_0 from pair-correlation functions have been applied to the data and both indicate little pressure dependence for n_0 within the limits of accuracy of this experiment, contrary to expectations based on the predicted dependence of the condensate fraction on density. This suggests either the prescriptions are wrong or that our understanding of the density dependence of the condensate fraction is quite incomplete. This lack of sensitivity is doubly surprising in the light of recent neutron scattering measurements of $n(p)$, the momentum-distribution function for liquid ^{4}He at various temperatures and densities by Mook.[35] $n(p)$ was discovered to be a strong function of density. Work by Sears *et al.*,[36] suggests that

$$\mathbf{n}(p)=n_0\delta(\mathbf{p})+(1-n_0)n^*(\mathbf{p})$$

with $n^*(p)$ the momentum distribution of the uncondensed atoms. Thus, the above result is indicative of strong changes in n_0 with density. Unfortunately, in that work values of $n^*(p)$ were not obtained and thus comparison to exact values of n_0 is not possible.

ACKNOWLEDGMENTS

We have benefited from conversations with E. C. Svensson, P. Sokol, and A. L. Fetter. This work was supported by the National Science Foundation, Grants No. DMR 79-09248 and No. DMR 83-18054. We are grateful to the University Computer Center for a grant of computer time.

*Present address: Hampshire College, Amherst, MA.

[1]D. G. Henshaw, Phys. Rev. **119**, 9 (1960).
[2]F. H. Wirth, D. A. Ewen, and R. B. Hallock, Phys. Rev. B **27**, 5530 (1983).
[3]H. N. Robkoff and R. B. Hallock, Phys. Rev. B **25**, 1572 (1982).
[4]H. N. Robkoff and R. B. Hallock, Phys. Rev. B **24**, 159 (1981).
[5]H. N. Robkoff, D. A. Ewen, and R. B. Hallock, Phys. Rev. Lett. **43**, 2006 (1979).
[6]V. F. Sears and E. C. Svensson, Phys. Rev. Lett. **43**, 2009 (1979).
[7]E. C. Svensson, V. F. Sears, A. D. B. Woods, and P. Martel, Phys. Rev. B **21**, 3638 (1980).
[8]E. C. Svensson and A. F. Murray, Physica **108B**, 1317 (1981).
[9]H. N. Robkoff, B. L. Weiss, and R. B. Hallock, Rev. Sci. Instrum. **52**, 1037 (1981).
[10]Rigaka/USA, Danvers, MA, Model RU-200PL.
[11]Brush Wallman Corp., Los Angeles, CA.
[12]Princeton Gamma Tech, Princeton, NJ, Model IG205-U.
[13]Siemens Co., Iselin, NJ, Type F.

[14]Rueter-Stokes Co., Cleveland, OH.
[15]A. G. Tweet, Phys. Rev. **93**, 15 (1954).
[16]D. L. Elwell and H. Meyer, Phys. Rev. **164**, 245 (1967).
[17]J. Maynard, Phys. Rev. B **14**, 3868 (1976).
[18]*Argon, Helium and The Rare Gases VI,* edited by G. A. Cook (Interscience, New York, 1961), p. 262.
[19]C. Tovard, D. Nicholas, and M. Ronault, J. Chim. Phys. **64**, 540 (1967).
[20]Y. K. Kim and M. Inokuti, Phys. Rev. **165**, 39 (1968).
[21]I. A. Blech and B. L. Averbach, Phys. Rev. **137A**, 1113 (1965).
[22]G. Galglione, G. L. Masserini, and L. Reatto, Phys. Rev. B **23**, 1129 (1981).
[23]O. Penrose, in *Proceedings of the International Conference on Low Temperature Physics,* edited by J. R. Dillinger (University of Wisconsin Press, Madison, 1958), p. 117.
[24]B. Mozer, L. A. DeGraaf, and B. LeNeindre, Phys. Rev. A **9**, 448 (1974).
[25]See AIP document no. PAPS PRBMD-35-116-37 for 37 pages of pair-correlation function values deduced from these structure factor measurements. Order by PAPS number and journal reference from American Institute of Physics, Physics Auxiliary Publication Service, 335 East 45th Street, New York, N.Y. 10017. The price is $1.50 for each microfiche (98 pages) or $5.00 for photocopies of up to 30 pages, and $0.15 for each additional page over 30 pages. Airmail additional. Make checks payable to the American Institute of Physics. Also reported in AIP document no. PAPS PRBMD-35-116-37 are values for the smoothed (fitted) structure factor on a useful momentum-transfer grid. Additional structure factor values deduced from a reanalysis of the work reported in Refs. 3 and 4 are also given there.
[26]G. J. Hyland, G. Rowlands, and F. W. Cummings, Phys. Lett. **31A**, 465 (1970).
[27]H. Frohlich, Phys. Kondens. Mater. **9**, 350 (1969).
[28]A. L. Fetter, Phys. Rev. B **23**, 2425 (1981).
[29]G. V. Chester and L. Rialto, Phys. Rev. B **22**, 5199 (1980).
[30]A. Griffin, Phys. Rev. B **22**, 5193 (1980).
[31]F. W. Cummings, G. J. Hyland, and G. Rowlands, Phys. Lett. **86A**, 370 (1981).
[32]W. L. MacMilan, Phys. Rev. **138A**, 842 (1965).
[33]V. I. Yukalov, Phys. Lett. **83A**, 26 (1981).
[34]See, for example, P. A. Whitlock, D. M. Ceperley, G. V. Chester, and M. H. Kalos, Phys. Rev. B **19**, 5598 (1979).
[35]H. A. Mook, Phys. Rev. Lett. **51**, 1454 (1983).
[36]V. F. Sears, E. C. Svensson, P. Martel, and A. D. B. Woods, Phys. Rev. Lett. **49**, 279 (1982).
[37]P. E. Sokol, R. O. Simmons, R. D. Hilleke, and D. L. Price (unpublished); P. E. Sokol (private communication).
[38]V. F. Sears, Phys. Rev. B **28**, 5109 (1983).
[39]R. McCarty, J. Phys. Chem. Ref. Data **2**, 923 (1973).
[40]R. A. Aziz, V. P. S. Nain, J. S. Carley, W. L. Taylor, and G. T. McConville, J. Chem. Phys. **70**, 4330 (1979).
[41]M. H. Kalos, M. A. Lee, and P. A. Whitlock, Phys. Rev. B **24**, 115 (1981).